

Electronic Supplementary Information

Bimetallic Silver nanoparticle-Gold nanocluster embedded composite for cancer theranostics

Deepanjalee Dutta,^a Amaresh Kumar Sahoo,^a Arun Chattopadhyay^{a,c*} and Siddhartha Sankar Ghosh^{a,b*}

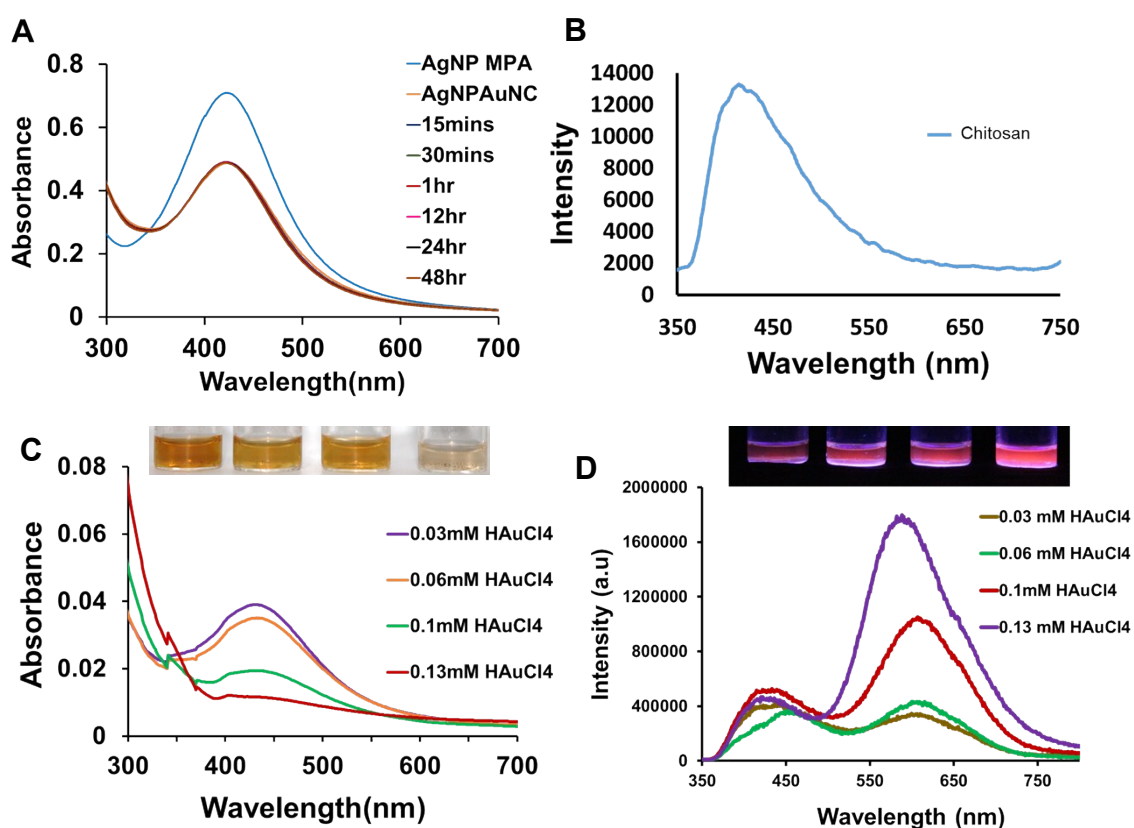


Figure S1. (A) Time dependent UV – Vis absorption spectra of the AgNP-AuNCs, (B) Emission spectra of control chitosan. ($\lambda_{\text{ex}} = 300$ nm), (C) UV-Vis absorption spectra of the AgNP-AuNCs with increasing concentration of H₂AuCl₄, corresponding images are given in the inset, (D) Emission spectra of the AgNP-AuNCs with increasing concentration of H₂AuCl₄, corresponding images are given in the inset. ($\lambda_{\text{ex}} = 300$ nm).

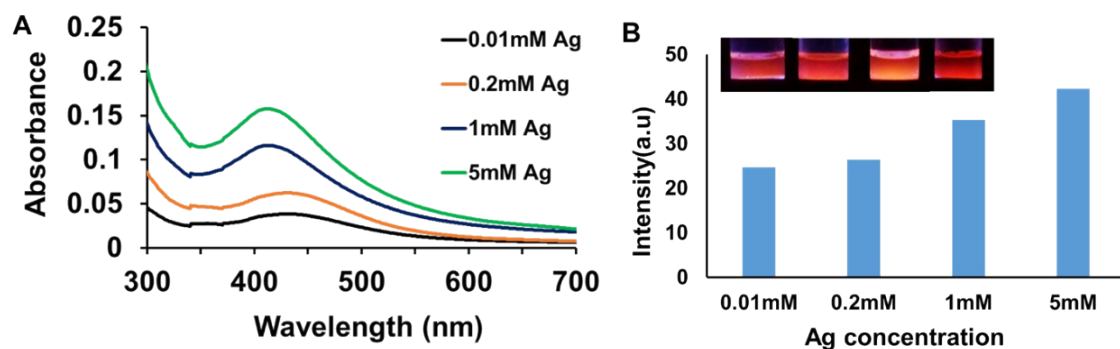


Figure S2. (A) UV-Vis absorption spectra of the AgNP-AuNCs with increasing amount of Ag. (B) Emission intensity of the AgNP-AuNCs with increasing concentration of Ag, corresponding images are given in the inset.

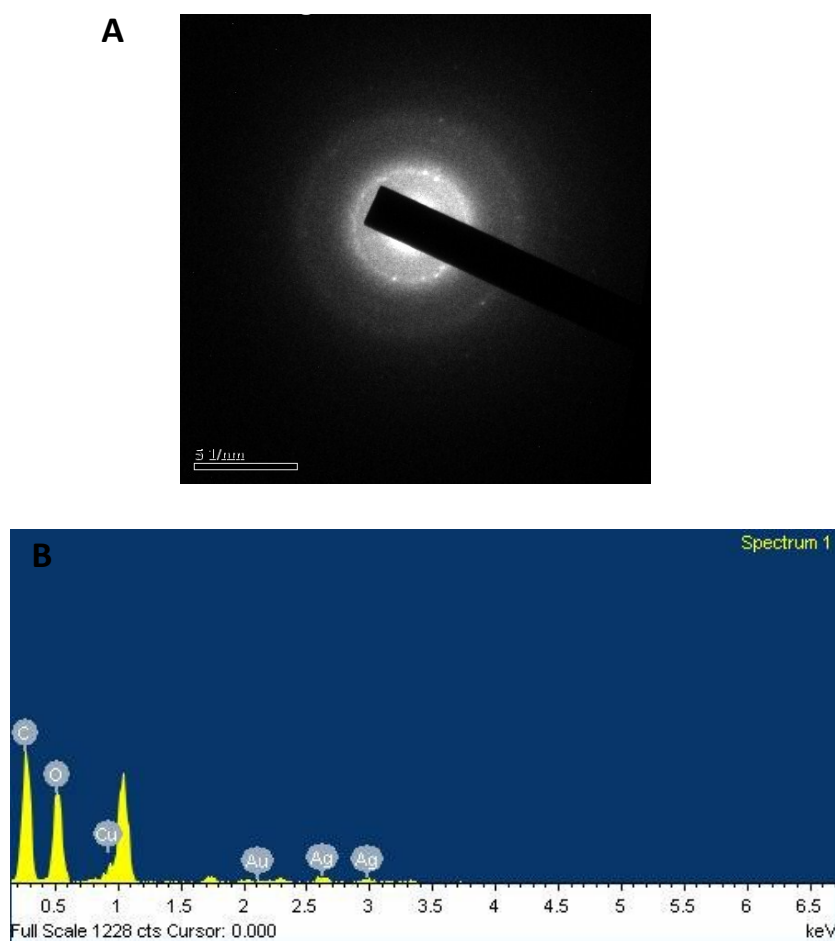


Figure S3.(A) SAED of AgNP-AuNCs, (B) EDX spectrum of the AgNP-AuNCs.

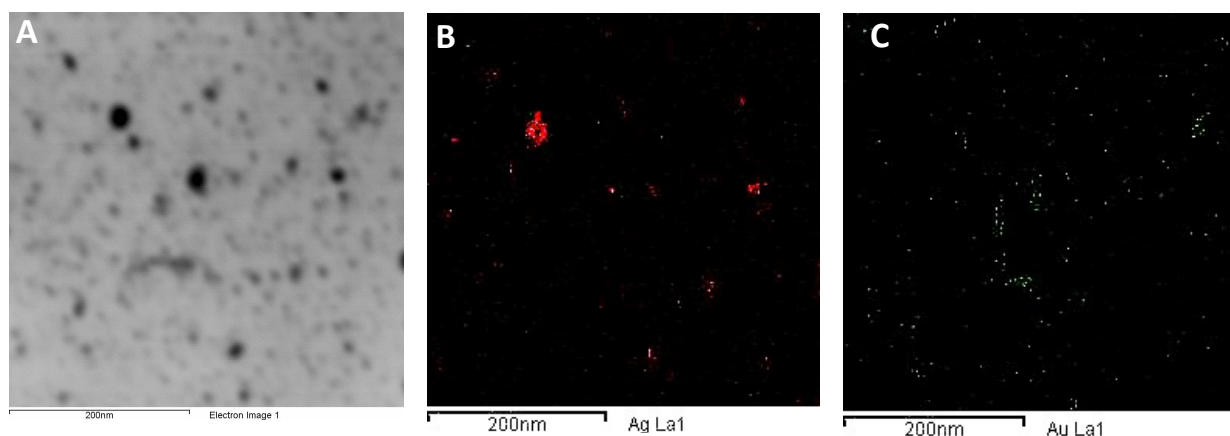


Figure S4. HAADF-STEM (BF) image of AgNP-AuNCs synthesized in chitosan matrix (A); EDX mapping image corresponding to Ag (B) and EDX mapping image corresponding to Au(C)

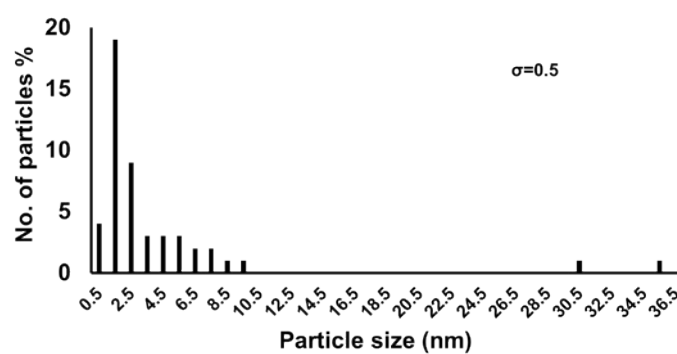
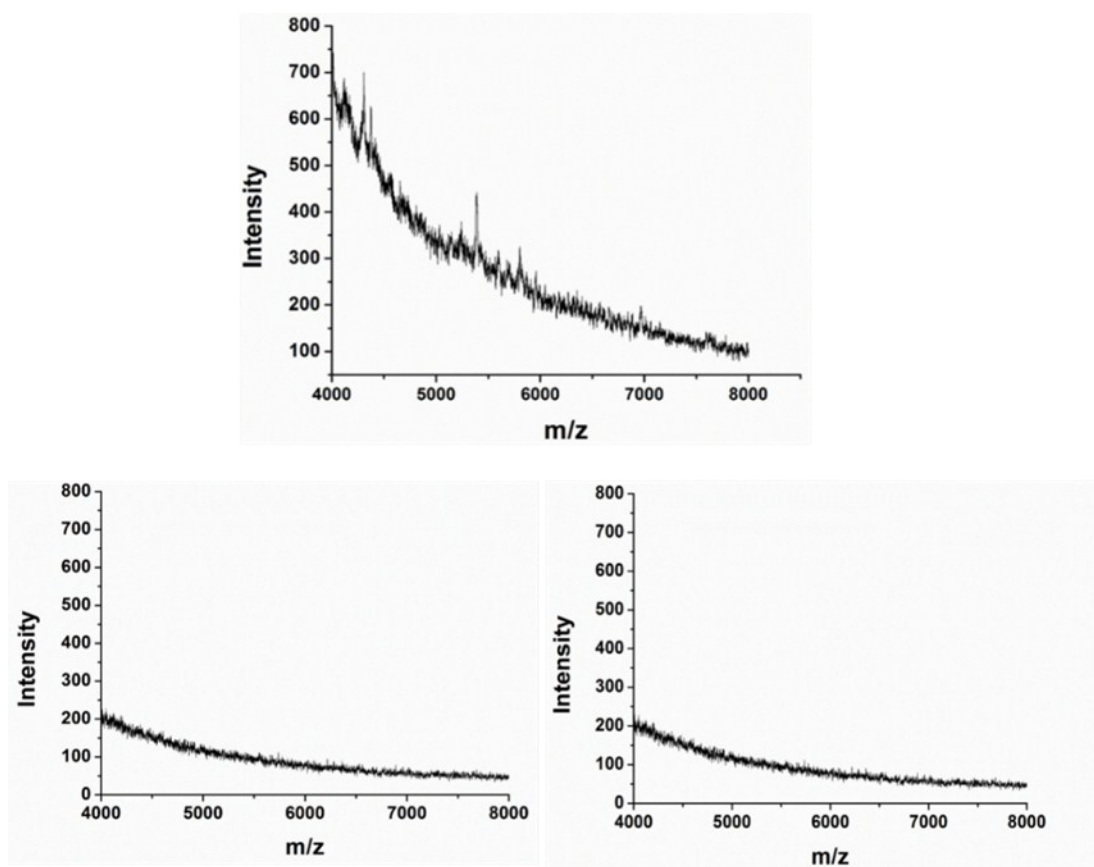


Figure S5. Particle size distribution of the AgNP-AuNCs as obtained from the TEM image in Figure 1(C).



FigureS6: MALDI-TOF analysis of (A) AgNP-AuNCs, (B) control AgNPs and (C) control chitosan.

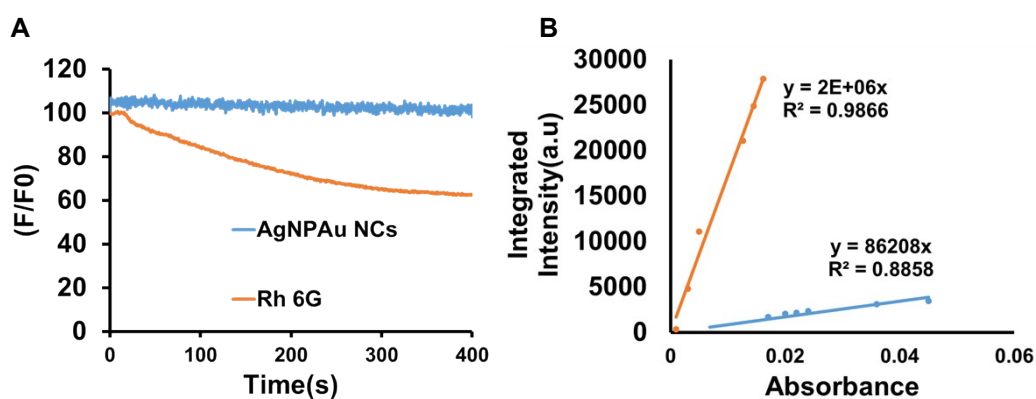


Figure S7. (A) Photostability of AgNP-AuNCs with respect to rhodamine 6G. (B) Quantum yield of AgNP-AuNCs with respect to quinine sulphate.

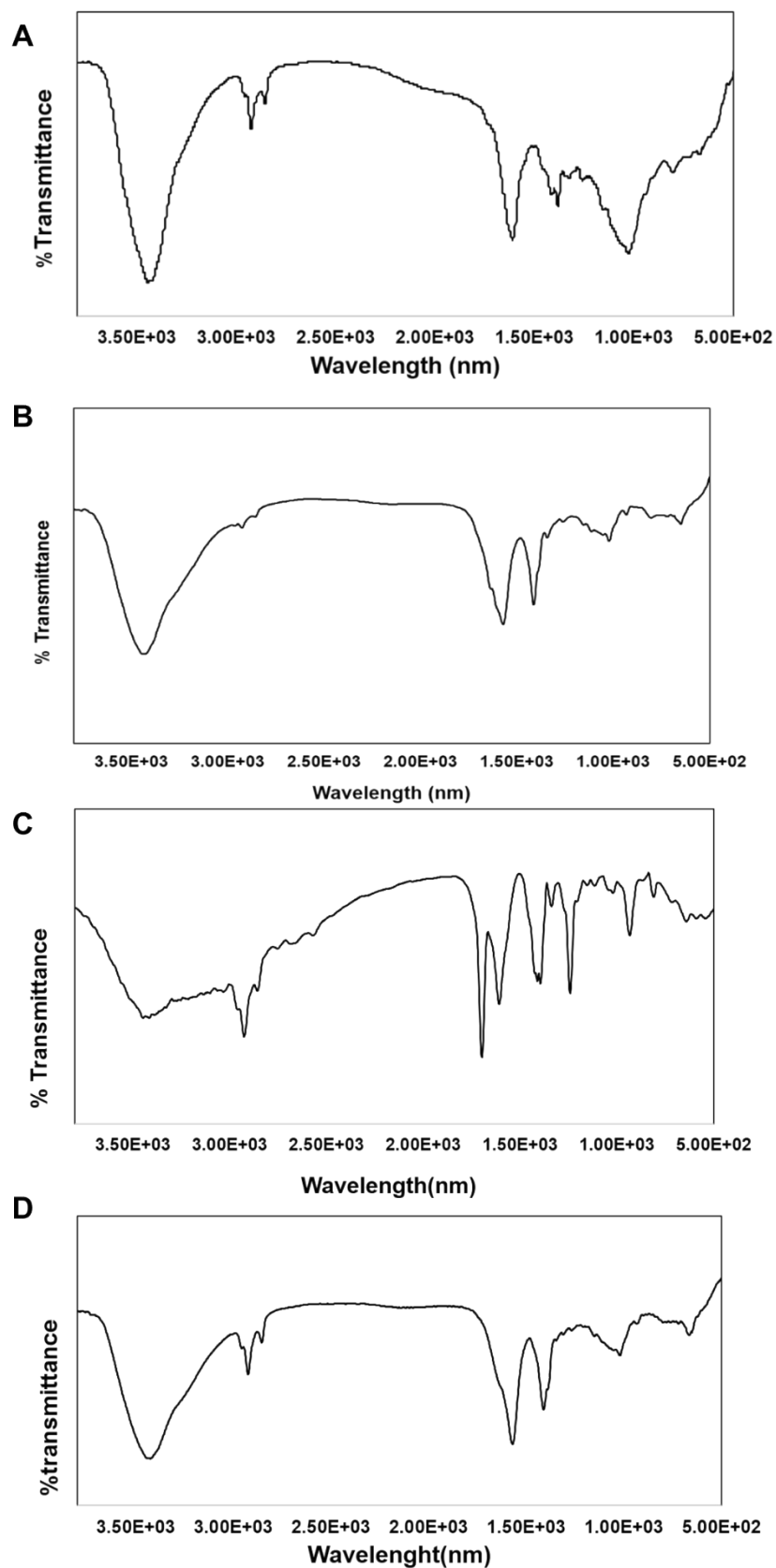


Figure S8. (A) FTIR spectrum of control chitosan (B) FTIR spectrum of AgNPs (chitosan

stabilized), (C) FTIR spectrum of free MPA, (D) FTIR spectrum of AgNP-AuNCs (chitosan stabilized).

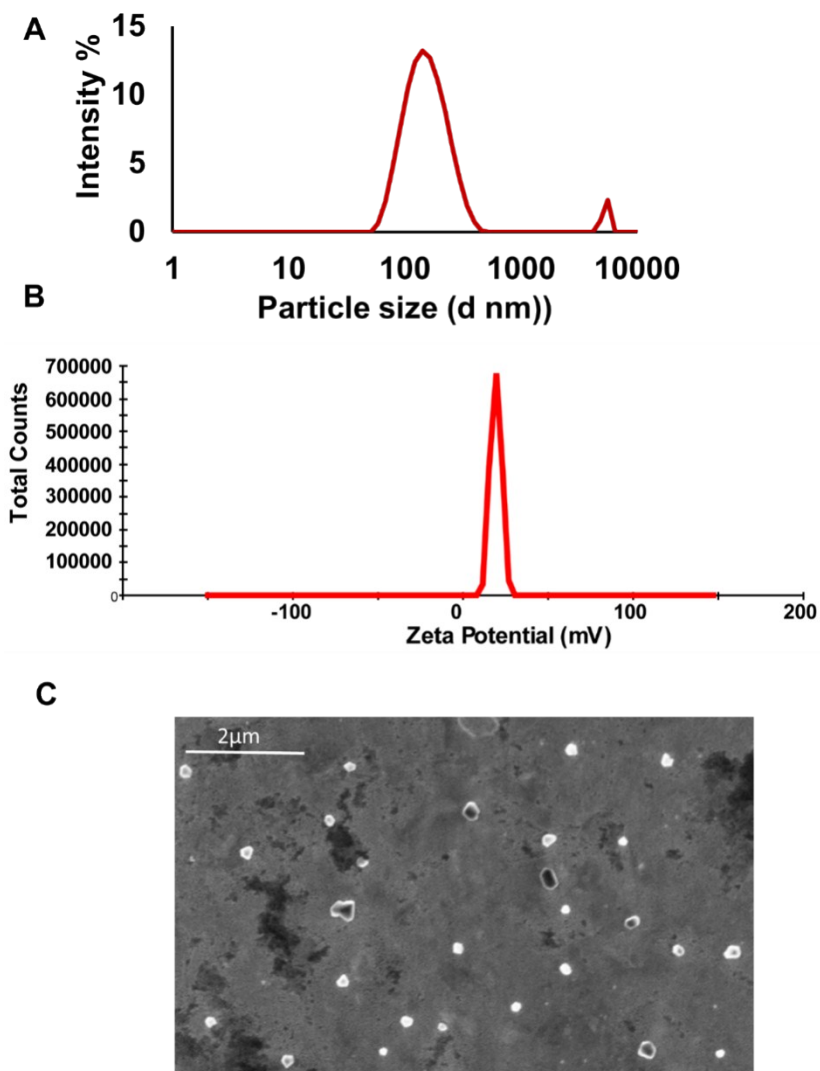


Figure S9. (A) Hydrodynamic particle size of composite NPs (AgNP-AuNC-CS NP). (B) Zeta potential distribution of composite NPs. (C) FESEM image of the composite NPs.

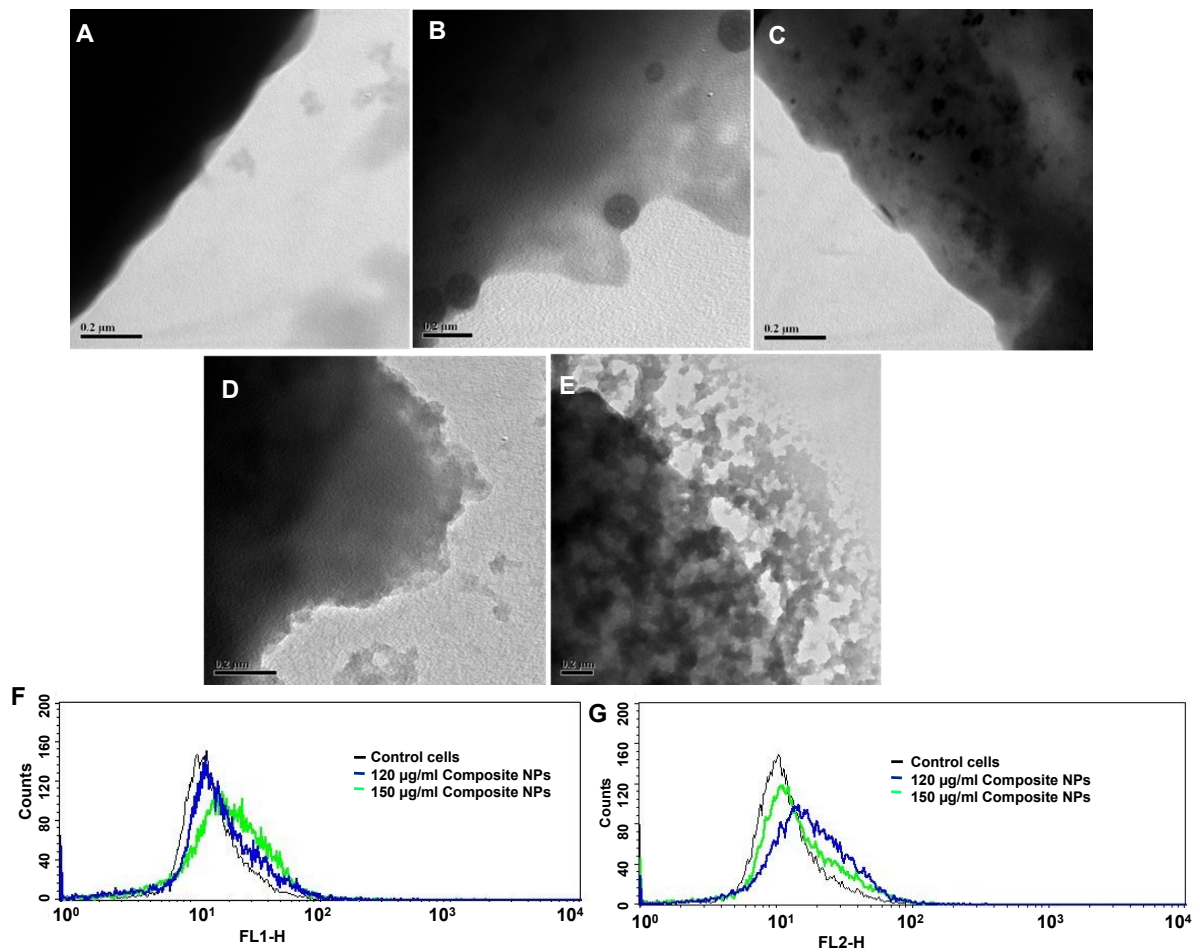


Figure S10. (A-E) Time dependent TEM analysis of HeLa cells treated with IC₅₀ dose of composite NPs for 1 h, 3 h, 6 h, 12 h, 24 h, respectively, at 0.2 μm scale. Extensions of plasma membrane at 3 h suggests endocytosis mediated uptake of composite NPs; membrane disruption at 24 h is visible. (F,G) FACS analysis of uptake of composite NPs in FL1-H and FL2-H, respectively.

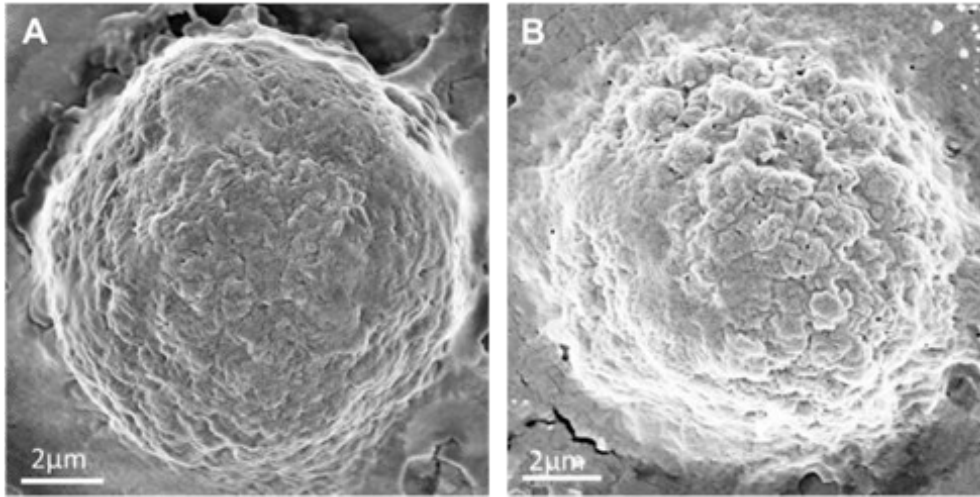


Figure S11: (A-B) FESEM images of control and composite NP_Δ treated HeLa cells. Scale bar is 2 μm .

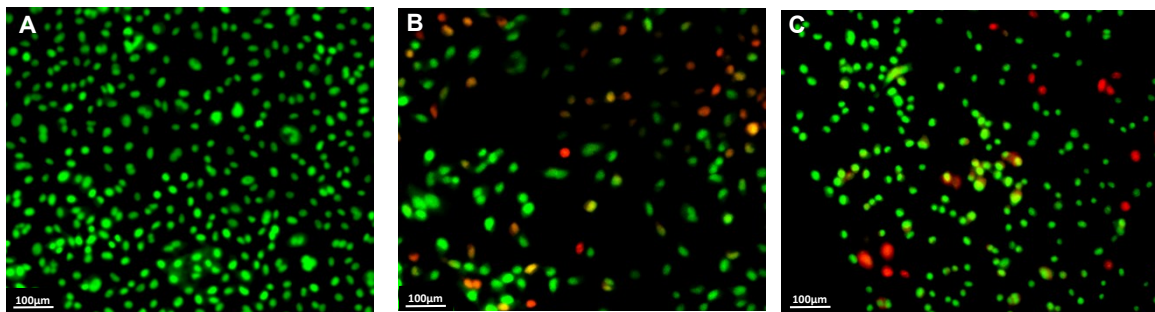


Figure S12. (A) EtBr/AO double staining of control HeLa cells, (B) composite NP_Δ treated (for 24 h at IC₅) HeLa cells, (C) AgNP_Δ only treated HeLa cells for 24 hrs at IC₅₀.

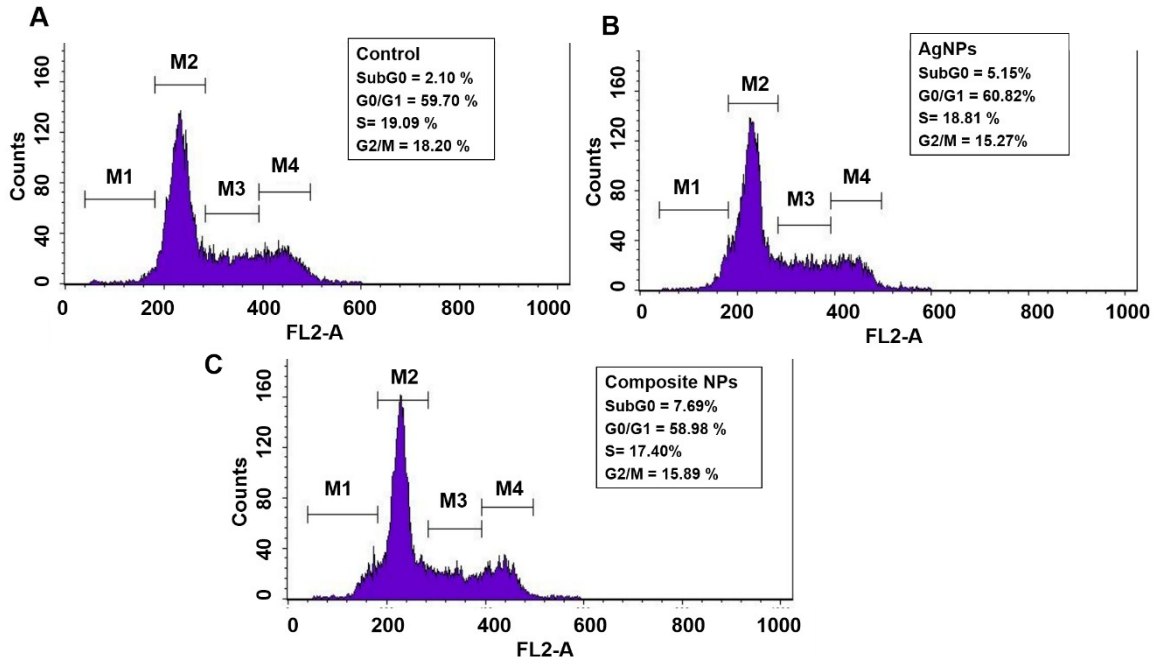


Figure S13. (A-C) Cell cycle analysis of control HeLa cells, AgNP_A treated HeLa Cells, composite NPs treated HeLa cells, respectively, for 24 h at IC₅₀.

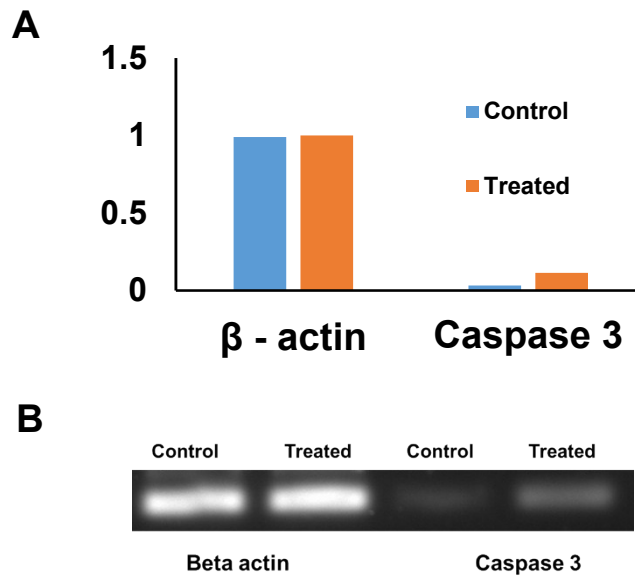


Figure S14. (A-B) Overexpression of Caspase 3 was observed from gene expression analysis of composite NP_A treated and control cells, taking β -actin as endogenous control.